AUDIER, M. & GUYOT, P. (1988). *Quasicrystalline Materials. Proceedings of the ILL/CODEST Workshop*, edited by C. JANOT & J. M. DUBOIS, pp. 181–194. Singapore: World Scientific.

BOYER, L. L. & BROUGHTON, J. Q. (1990). *Phys. Rev. B*, **42**, 11461–11468.

CAHN, J. W., GRATIAS, D. & MOZER, B. (1988a). *J. Phys. (Paris)*, **49**, 1225–1233.

CAHN, J. W., GRATIAS, D. & MOZER, B. (1988b). *Phys. Rev. B*, **38**, 1638–1642.

CHENG, Y. F., HANSEN, V., GJØNNES, J. & WALLENBERG, R. L. (1992). *J. Mater. Res.* **7**, 3235–3241.

CHENG, Y. F., PAN, G. Z. & LI, F. H. (1992). *Phys. Status. Solidi B*, **170**, 47–55.

COOPER, M. (1967). *Acta Cryst.* **23**, 1106–1107.

COOPER, M. & ROBINSON, K. (1966). *Acta Cryst.* **20**, 614–617.

DMITRIENKO, V. E. (1990). *J. Phys. (Paris)*, **51**, 2712–2732.

DUNEAU, M. & OGUEY, C. (1989). *J. Phys. (Paris)*, **50**, 135–146.

ELSER, V. (1985). *Phys. Rev. B*, **32**, 4892–4898.

ELSER, V. (1986). *Acta Cryst.* A**42**, 36–43.

ELSER, V. & HENLEY, C. L. (1985). *Phys. Rev. Lett.* **55**, 1883–1886.

GUYOT, P. & AUDIER, M. (1985). *Philos. Mag.* B**52**, L15–L19.

HANSEN, V. & GJØNNES, J. (1992). *Micron Microsc. Acta*, **23**, 175–176.

HANSEN, V. & GJØNNES, J. (1994). In preparation.

HANSEN, V., GJØNNES, J. & ANDERSSON, B. (1989). *J. Mater. Sci. Lett.* **8**, 823–826.

HENLEY, C. L. & ELSER, V. (1986). *Philos. Mag.* B**53**, L59–L66.

ISHII, Y. (1989). *Phys. Rev. B*, **39**, 11862–11871.

JANSSEN, T. & JANNER, A., (1987). *Adv. Phys.* **36**, 519–624.

KRAMER, P. & HAASE, R. W. (1989). In *Aperiodicity and Order* 2: *Introduction to the Mathematics of Quasicrystals*, edited by MARKO V. JARIĆ. New York: Academic Press.

LI, F. H. & CHENG, Y. F. (1990). *Acta Cryst.* A**46**, 142–149.

MACKAY, A. L. (1982). *Physica. (Utrecht)*, A**114**, 609–613.

MAI, Z. H., TAO, S. Z., ZHANG, B. S. & ZENG, L. Z. (1989). *J. Phys. Condens. Matter*, **1**, 2465–2471.

NIIZEKI, K. (1992). *J. Phys. A*, **25**, 1843–1854.

PAN, G. Z., CHENG, Y. F. & LI, F. H. (1990). *Phys. Rev. B*, **51**, 3401–3405.

PENROSE, R. (1974). *Bull. Inst. Math. Appl.* **10**, 266–271.

SHECHTMAN, D., BLECH, I., GRATIAS, D. & CAHN, J. W. (1984). *Phys. Rev. Lett.* **53**, 1951–1953.

SOCOLAR, J. E. S., STEINHARDT, P. J. & LEVINE, D. (1985). *Phys. Rev. B*, **32**, 5547–5550.

YANG, Q. B. & KUO, K. H. (1986). *Philos. Mag.* B**53**, L115–L121.

The Temperature Dependence of the Reflection Intensities of the Modulated Composite Structure Hg$_{0.776}$(BEDT-TTF)SCN

BY MARK R. PRESSPRICH, CORNELIS VAN BEEK* AND PHILIP COPPENS

Department of Chemistry, State University of New York at Buffalo, Buffalo, NY 14214, USA

Abstract

The temperature dependence between 30 and 300 K of the intensities of 24 reflections of the column-composite structure Hg$_{0.776}$(BEDT-TTF)SCN [Wang, Beno, Carlson, Thorup, Murray, Porter, Williams, Maly, Bu, Petricek, Cisarova, Coppens, Jung, Whangbo, Schirber & Overmyer (1991). *Chem. Mater.* **3**, 508–513; BEDT-TTF = 3,4,3′,4′-bis(ethylenedithio)-2,2′,5,5′-tetrathiafulvalene] has been analyzed in terms of a model including phason temperature factors. The temperature dependence of the main and first-order satellite reflections is reasonably well reproduced in a refinement with 236 observations and four variables. The results are interpreted in terms of a temperature independence of the static displacement amplitudes. The room-temperature r.m.s. phason fluctuations of the mercury sublattice are 50 (2)°. This value implies that the *mean* mercury displacement amplitude will increase by ~60% on

lowering of the temperature to within the liquid-helium range. The thermal contraction on cooling is the same for the two sublattices.

Introduction

For a modulated crystal, the usual description of the effect of atomic thermal motion on the reflection intensities must be modified by the introduction of Debye–Waller factors that vary from unit cell to unit cell along the modulation-vector direction, as the translational symmetry in this direction no longer exists. The temperature-factor modulation can be described by a Fourier series, the form of which follows from superspace-group theory (Yamamoto, 1982).

In addition, the phase and amplitude of the modulation can fluctuate. Such modes are thermally excited at quite low temperatures. The temperature-factor theory of phasons and amplitudons was introduced by Overhauser (1971) and further developed by Axe (1980). Perez-Mato & Madariaga (1990)

---

* Current address: University of Twente, The Netherlands.

established the relation between phase and amplitude fluctuations and the modulation of the atomic thermal parameters using the Landau theory of phase transitions.

In composite crystals, the modulation is not caused by the condensation of a soft phonon but arises from the coexistence in one crystal of two sublattices with different periodicities in at least one direction (Janner & Janssen, 1980; Petricek, Maly, Coppens, Bu, Cisarova & Frost-Jensen, 1991). As the temperature dependence of the reflection intensities of composite structures remains unexplored, we have measured a number of reflections of the composite crystal $Hg_{0.776}(BEDT\text{-}TTF)SCN$ [BEDT-TTF, abbreviated as ET, is 3,4;3',4'-bis(ethylenedithio)-2,2',5,5'-tetrathiafulvalene] (Wang, Beno, Carlson, Thorup, Murray, Porter, Williams, Maly, Bu, Petricek, Cisarova, Coppens, Jung, Whangbo, Schirber & Overmyer, 1991). One of the sublattices of this crystal is particularly simple, with only a single Hg atom in its unit cell. The other sublattice contains SCN^- ligands and partially oxidized ET molecules. Without the modulation, the intersublattice Hg–S distances show very large variations. The large modulational displacements of the mercury and SCN^- moieties are such that chemically reasonable intersublattice Hg–S bond lengths occur and the mercury valency remains quite constant along the incommensurate direction (Coppens, Cisarova, Bu & Sommer-Larsen, 1991).

Experimental

Synthesis

$(ET)Hg_{0.776}(SCN)_2$ was prepared as described in the literature (Wang *et al.*, 1991).

X-ray analysis

Intensity data were collected at between 30 and 300 K on a Huber diffractometer equipped with a Displex cryostat and a high-stability mounting device (Henricksen, Larsen & Rasmussen, 1986; Graafsma, Sagerman & Coppens, 1991). 24 reflections were collected with Mo $K\alpha$ radiation ($\lambda = 0.71069$ Å) in the range $0.11 < \sin\theta/\lambda < 0.43$ Å^{-1}. They are listed in Table 1. One of the reflections, 2010, is a primary reflection of both lattices,* seven reflections with indices $hl l0$ are primary reflections of the (ET)SCN lattice and first-order satellites of the mercury lattice, 13 reflections with indices $h0 l1$ are primary reflections of the mercury lattice and first-order satellites of the (ET)SCN lattice and three reflections with

---

* The *b*-axis direction is common to both sublattices, $hkl0$ reflections are main reflections of the (ET)SCN lattice, $h0lm$ reflections are the main reflections of the mercury lattice.

Table 1. *List of Miller indices of the reflections, calculated component structure factors (excluding the anomalous scattering contribution) and agreement factors for the refinement of the temperature dependence as described in the text*

Reflection				$F_{Hg}^{298\ K}$	$F_{(ET)SCN}^{298\ K}$	$\sin\theta/\lambda$ (Å^{-1})	$wR(Y^{1/2})$
2	0	1	0	45.4	70.8	0.183	0.07
0	1	0	0	4.0	124.5	0.141	0.07
-2	1	2	0	22.0	-15.0	0.159	0.08
-2	1	4	0	26.4	4.4	0.171	0.05
-3	1	3	0	26.8	-9.5	0.224	0.06
-5	1	4	0	24.7	19.1	0.337	0.07
-5	1	6	0	26.2	39.7	0.380	0.09
-4	-1	6	0	-8.9	-34.2	0.430	0.08
0	0	1	1	50.1	-2.4	0.110	0.05
0	0	3	1	48.3	-5.4	0.114	0.06
-1	0	4	1	46.1	0.6	0.119	0.07
0	0	2	1	49.6	-2.8	0.124	0.07
-2	0	2	1	41.1	-5.7	0.153	0.07
-2	0	4	1	38.2	-3.1	0.157	0.07
-3	0	3	1	44.9	-14.9	0.224	0.09
0	0	11	1	26.4	9.3	0.284	0.04
2	0	5	1	34.3	-1.1	0.287	0.05
2	0	6	1	32.7	-2.1	0.301	0.05
3	0	3	1	28.1	-0.2	0.345	0.10
3	0	4	1	27.6	0.7	0.355	0.11
3	0	5	1	26.8	0.5	0.367	0.11
-2	1	2	1	18.2	3.2	0.223	0.08
-2	1	4	1	21.6	6.6	0.229	0.07
-3	1	3	1	22.6	1.0	0.257	0.05

indices $hl l1$ are first-order satellites of both lattices. Overall, 441 reflection intensities were measured, of which 260 were unique. The data were scaled for $\sim 40\%$ crystal decay during data collection by periodic (re-)collection of reflections at 150 and 300 K.

The phason model

The instantaneous position of an atom in a modulated crystal, u_l, can be expressed as $x_l = l + \langle u_l \rangle + \delta u_l$, where l describes its position in the absence of the modulation and $l + \langle u_l \rangle$ is the mean or time-averaged position of the atom in the presence of the displacive modulation. The displacement u_l depends on the amplitude A and the phase θ_l of one or more modulation waves. For a single sinusoidal modulation wave,

$$u_l = A \cos\theta_l, \tag{1}$$

with $\theta_l = q \cdot l - \theta_0$, where q is the wave vector of the modulation and θ_0 is the value of the phase in the absence of phason excitations.

When the phasons are excited and phase fluctuations occur, the time-averaged displacement is given by (Axe, 1980)

$$\langle u_l \rangle = \eta \cos\theta_l, \tag{2}$$

where η, the time-averaged amplitude vector of the modulation, is related to the static amplitude vector A by

$$\eta = A \langle \cos \delta\varphi \rangle. \tag{3}$$

$\delta\varphi$ is the instantaneous fluctuation of the phase of the displacement wave. η generally has a smaller magnitude than A, as illustrated in Fig. 1.

In the absence of amplitude modulations, the instantaneous change in the displacement of the atom can be written as[†]

$$\delta u_l = A[(\cos \varphi_l - \langle \cos \delta\varphi \rangle) \cos \theta_l + \sin \varphi_l \sin \theta_l]. \quad (4)$$

With the inclusion of the effect of the phase fluctuations and the omission, for the moment, of the Debye–Waller temperature factor, the contribution of atom ν to the time-averaged structure factor is given by

$$F_\nu(H) = f_\nu(H) \exp [ni(\pi - \theta_{0,\nu})] \exp (2\pi i H \cdot r_\nu^0)$$
$$\times J_n(2\pi H \cdot A_\nu)\langle\exp (in\delta\varphi_l)\rangle, \quad (5)$$

with $H = ha^* + kb^* + lc^* + nq$. To simplify the expressions, we discuss the case of a single atom with unit scattering power, located at the origin of the unit cell. For this case, (5) becomes

$$F(H) = \exp [ni(\pi - \theta_0)]J_n(2\pi H \cdot A)\langle\exp (in\delta\varphi_l)\rangle. \quad (6)$$

If the phase fluctuations $\delta\varphi$ have a Gaussian distribution, the last term in (6) can be written as

$$\langle\exp (in\delta\varphi_l)\rangle = 1 - (n^2/2)\langle\delta\varphi^2\rangle + (n^4/24)\langle\delta\varphi^4\rangle, \quad (7a)$$

which, for small values of the phase fluctuations, can be approximated by

$$\langle\exp (in\delta\varphi_l)\rangle \simeq \exp [- (n^2/2)\langle\delta\varphi^2\rangle], \quad (7b)$$

[†] We have omitted the effect of amplitudons, which are especially important in the vicinity of phase transitions representing the onset of a change in the modulation pattern. No such transitions occur in the composite crystals studied here.
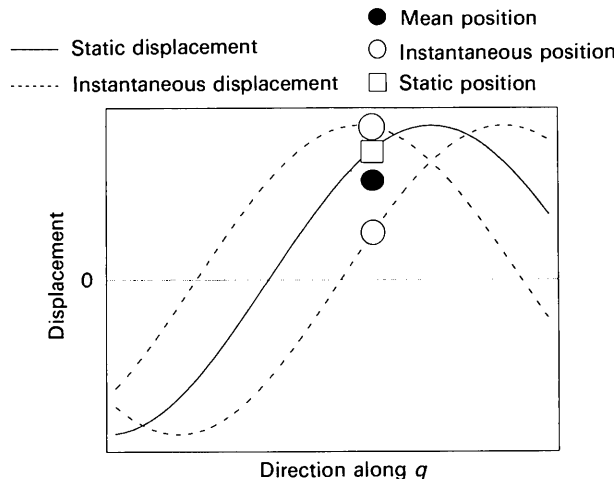

—— Static displacement   ● Mean position
······ Instantaneous displacement   ○ Instantaneous position
     □ Static position

Fig. 1. Illustration of the apparent decrease of the modulation amplitude owing to the phase fluctuations of the modulation wave.

which gives

$$F(H) = \exp [ni(\pi - \theta_0)]J_n(2\pi H \cdot A)$$
$$\times \exp [- (n^2/2)\langle\delta\varphi^2\rangle]. \quad (8)$$

While (8) has been used in the present analysis of the temperature dependence of the reflection intensities, it is useful to express the structure factor in terms of the mean amplitude η, which defines the mean positions of the atoms in the crystal. For small values of η,

$$F(H) = \exp [ni(\pi - \theta_0)]J_n(2\pi H \cdot \eta)$$
$$\times [J_n(2\pi H \cdot A)/J_n(2\pi H \cdot \eta)]$$
$$\times \exp [-(n^2/2)\langle\delta\varphi^2\rangle]. \quad (9)$$

As the nth-order Bessel function is given by the expansion

$$J_n(x) = [x^n/2^n\Gamma(n + 1)]\{1 - [x^2/2(2n + 2)]$$
$$+ [x^4/2 \times 4(2n + 2)(2n + 4)] - ...\}, \quad (10)$$

where $\Gamma(n + 1)$ is the gamma function equal to $n!$ for positive integer n, for small x and y:

$$J_n(x)/J_n(y) \simeq (x/y)^{|n|} \exp [(y^2 - x^2)/2(2|n| + 2)]. \quad (11)$$

This expression is equally valid for negative values of n, as $J_{-n}(x) = (-1)^n J_n(x)$. Thus,

$$J_n(2\pi H \cdot A)/J_n(2\pi H \cdot \eta)$$
$$\simeq (H \cdot A/H \cdot \eta)^{|n|}$$
$$\times \exp \{[(2\pi H \cdot \eta)^2 - (2\pi H \cdot A)^2]/2(2|n| + 2)\}$$
$$= (A/\eta)^{|n|} \exp \{(2\pi H \cdot \eta)^2/2(2|n| + 2)[1 - (A/\eta)^2]\}$$
$$\simeq \exp [(|n|/2)\langle\delta\varphi^2\rangle]$$
$$\times \exp \{[- (2\pi H \cdot \eta)^2/2(2|n| + 2)]\langle\delta\varphi^2\rangle\}, \quad (12)$$

where we have made use of the collinearity of η and A and the expressions

$$A/\eta = 1/\langle\cos \delta\varphi\rangle \simeq 1/(1 - \langle\delta\varphi^2\rangle/2) \simeq 1 + (\langle\delta\varphi^2\rangle/2)$$

and

$$\exp (\langle\delta\varphi^2\rangle/2) \simeq 1 + (\langle\delta\varphi^2\rangle/2).$$

With this substitution, the expression for the structure factor becomes

$$F(H) = \exp [ni(\pi - \theta_0)]J_n(2\pi H \cdot \eta) \exp (- \{(n^2/2)$$
$$- (|n|/2) + [1/(|n| + 1)](2\pi H \cdot \eta/2)^2\}\langle\delta\varphi^2\rangle). \quad (13)$$

Expression (13) reverts to the equation given by Axe (1980) if the $(2\pi H \cdot \eta/2)^2$ term is small and can be neglected. As it includes a higher-order term, its range of validity will be larger than that of the expression given by Axe.

Determination of Debye–Waller and phason temperature factors by temperature-dependent experiments

For a crystal composed of two incommensurate composite lattices a and b, the structure factor can be expressed as

$$F = F_a + F_b. \tag{14}$$

If phasons are excited, they will contribute to the temperature dependence of the component structure factors, F_a and F_b.

The mean amplitude η is expected to vary through its phason dependence. We make the assumptions that the static amplitude A is independent of temperature and that the temperature dependence of each lattice is characterized by a single phason and a single isotropic Debye–Waller factor.

We may then write

$$F(T) = F_a^o \exp(\Delta b_a) + F_b^o \exp(\Delta b_b), \tag{15}$$

where $F_i^o = F_i(T_o)$ and

$$\Delta b_i(T) \equiv b_i(T) - b_i(T_o). \tag{16}$$

with the effect of phasons included according to (8),

$$b_i(T) = -(\sin^2 \theta / \lambda^2) B_i(T) - (n_i^2/2)\langle \delta \varphi_i^2(T) \rangle. \tag{17}$$

For temperatures larger than the Debye temperature, $\Delta B = B(T) - B(T_o)$ is proportional to ΔT. As the phasons are low-frequency modes, we can assume that phase fluctuations have a similar linear dependence, thus

$$\Delta b_i(T) = (\sin^2 \theta / \lambda^2) c_i^D \Delta T - (n_i^2/2) c_i^P \Delta T, \tag{18}$$

where the c_i's are the proportionality constants defined as $\Delta B / \Delta T$. In the absence of static disorder and neglecting zero-point vibrations, $c_i^D = B_i(T)/T$ and $c_i^P = \langle \delta \varphi_i^2(T) \rangle / T$.

We may eliminate the scale factor s defined by

$$I_o(\mathbf{H}) = s|F_c|^2 \tag{19}$$

by dividing the intensity at temperature T by the intensity at a reference temperature T_r: $Y_o(T) = I_o(T)/I_o(T_r)$.

The four parameters c_a^P, c_a^D, c_b^P and c_b^D can then be obtained by minimizing $\Sigma w(Y_o - Y_c)^2$, where

$$w = I_0^2(T_r)/\{\sigma^2[I_o(T)] + [Y_o(T)]^2 \sigma^2[I_o(T_r)] + xY_o^2\} \tag{20}$$

and

$$Y_c(T) = \{|F_a^o \exp[\Delta b_a(T)] + F_b^o \exp[\Delta b_b(T)]|^2\}$$
$$\times \{|F_a^o \exp[\Delta b_a(T_r)] + F_b^o \exp[\Delta b_b(T_r)]|^2\}. \tag{21}$$

The additional term xY_o^2 in the denominator of (20) allows for errors in the data set that are proportional to the measured signal $Y_o(T)$, in analogy to the procedure commonly used in structure refinement.

Application to Hg$_{0.776}$(ET)SCN

For Hg(ET)SCN, the two sublattices a and b correspond to a simple one-atom Bravais lattice containing mercury and a lattice containing the remaining atoms.

Fig. 2 shows the temperature dependence of the magnitudes of the modulation vectors, $|q_{Hg}|$ and $|q_{(ET)SCN}|$. The two sublattices and therefore the two modulation vectors are related by an interlattice matrix as discussed by Petricek et al. (1991). Fig. 3 shows the temperature dependence of the sublattice volumes. While the mercury and (ET)SCN lattices each decrease in volume, their ratio remains constant. Since the crystal stoichiometry is determined by this ratio, this must be the case unless vacancies occur in one of the component lattices.

The structure factors $F_a^o = F_{Hg}^{298 \ K}$ and $F_b^o = F_{(ET)SCN}^{298 \ K}$ needed for the evaluation of (21) were taken from the known structure (Wang et al., 1991) and are listed in Table 1. The calculated values of Y_c were fit to the multiple temperature reflection data
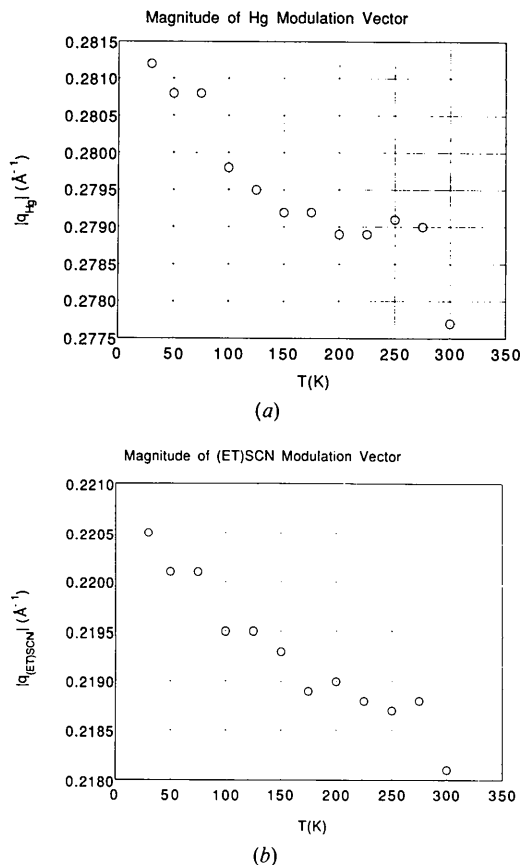
Fig. 2. Temperature dependence of the magnitude of the modulation vectors of the two sublattices: (a) mercury lattice; (b) (ET)SCN lattice.

by a linearized least-squares procedure, with the Debye–Waller and phason parameters of each substructure according to (18) as variables.

In the refinement, mean modulation amplitudes from the room-temperature study are used as an approximation to the static amplitudes **A**. For the mercury lattice, the amplitude of the large first-order harmonic terms was used. The Cartesian components are $A_x = 0.24$, $A_y = 0.01$ and $A_z = 0.27$ Å. For the (ET)SCN lattice, the translational displacive components were used, which are $A_x = 0.02$, $A_y = 0.01$ and $A_z = 0.10$ Å.

The four temperature parameters were refined with different values of the proportionality factor x in (20) against a total of 236 observations [24 data were used for $I_o(T_r)$]. The agreement factors for each of the 24 reflections are listed in the last column of Table 1. The refined values of the variables and overall agreement factors are listed in Table 2. Figs. 4(a)–(d) show the results for 2010, a primary Hg–primary (ET)SCN reflection; for $\overline{3}031$, a primary Hg–first-order (ET)SCN reflection; for $\overline{2}120$, a first-

Table 2. *Parameter values and overall agreement factors for the refinement of the temperature dependence of the reflection intensities*

Number of observations	236
Number of variables	4
$c^D_{Hg} = \Delta B_{Hg}/\Delta T$ (Å^2 K^{-1})	0.0083 (11)
$c^D_{(ET)SCN} = \Delta B_{(ET)SCN}/\Delta T$ (Å^2 K^{-1})	0.0072 (17)
$c^P_{Hg} = \Delta\langle\delta\varphi^2\rangle_{Hg}/\Delta T$ (rad^2 K^{-1})	0.0026 (2)
$c^P_{(ET)SCN} = \Delta\langle\delta\varphi^2\rangle_{(ET)SCN}/\Delta T$ (rad^2 K^{-1})	0.0000 (8)
x	1.9×10^{-5}
$wR(Y) \equiv [\Sigma w(Y_o - Y_c)^2/\Sigma w Y_o^2]^{1/2}$	0.14
$wR(Y^{1/2}) \equiv [\Sigma w'(Y_o^{1/2} - Y_c^{1/2})^2/\Sigma w' Y_o]^{1/2}$ with $w' = 4Y_o w$	0.069

order Hg–primary (ET)SCN reflection; and for $\overline{3}131$, a first-order Hg–first-order (ET)SCN reflection. As shown in Fig. 4(c) for the $\overline{2}120$ reflection, a refinement based on a two-parameter Debye–Waller model excluding the phason contribution is completely unsatisfactory.

The mercury parameters c^D_{Hg} and c^P_{Hg} resulting from the fit are insensitive to x, varying by much less than their e.s.d.'s for large variations in x. The (ET)SCN parameters are, on the other hand, quite sensitive. For example, with $x = 0.0$ the four temperature parameters refine to $c^D_{Hg} = 0.0083$ (14) Å^2 K^{-1}, $c^D_{(ET)SCN} = 0.0142$ (15) Å^2 K^{-1}, $c^P_{Hg} = 0.0027$ (3) rad^2 K^{-1} and $c^P_{(ET)SCN} = -0.0026$ (11) rad^2 K^{-1} with $wR(Y) = 0.15$. The apparent large negative correlation between the two (ET)SCN temperature parameters appears unjustified by the small correlation coefficient of -0.26 ($x = 1.9 \times 10^{-5}$) between these parameters. The sensitivity of the (ET)SCN parameters to the refinement conditions precludes the attachment of much physical significance to their refined values.

Fig. 3. Temperature dependence of the sublattice volumes: (a) mercury cell; (b) (ET)SCN cell.

Discussion

The results show that the data can be fitted reasonably well by the model in which the temperature dependence is described by one Debye–Waller and one phason temperature parameter for each of the sublattices of the composite structure and in which all four temperature parameters are proportional to the absolute temperature. Only the phason temperature parameter for the mercury sublattice is significantly different from zero.

Further support for the temperature independence of **A** in the mercury sublattice is provided by comparing the derived Debye–Waller coefficient, c^D_{Hg}, to the Debye–Waller factor determined in the room-temperature structure analysis. If the structure is assumed to be statically ordered and zero-point motion is neglected, then $c^D_{Hg} = 0.0083$ (11) Å^2 K^{-1} corresponds to a room-temperature isotropic temperature factor of $B_{Hg} = c^D_{Hg} \times 300$ K $= 2.5$ (3) Å^2.
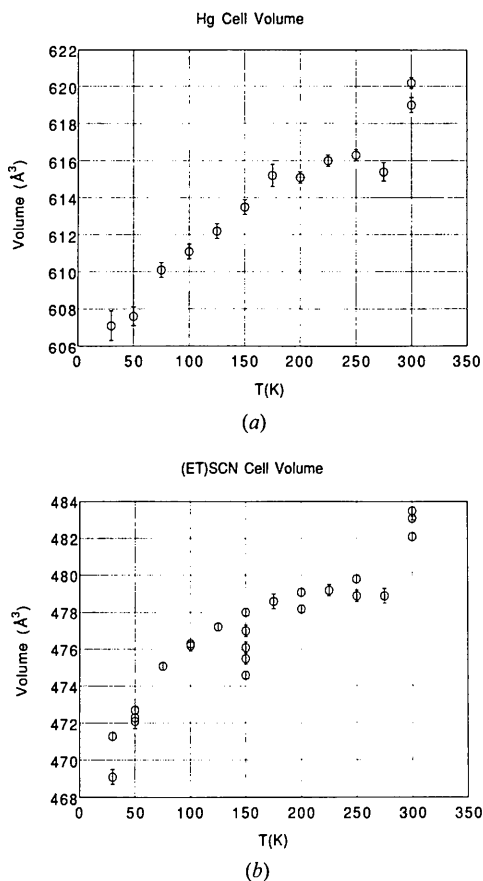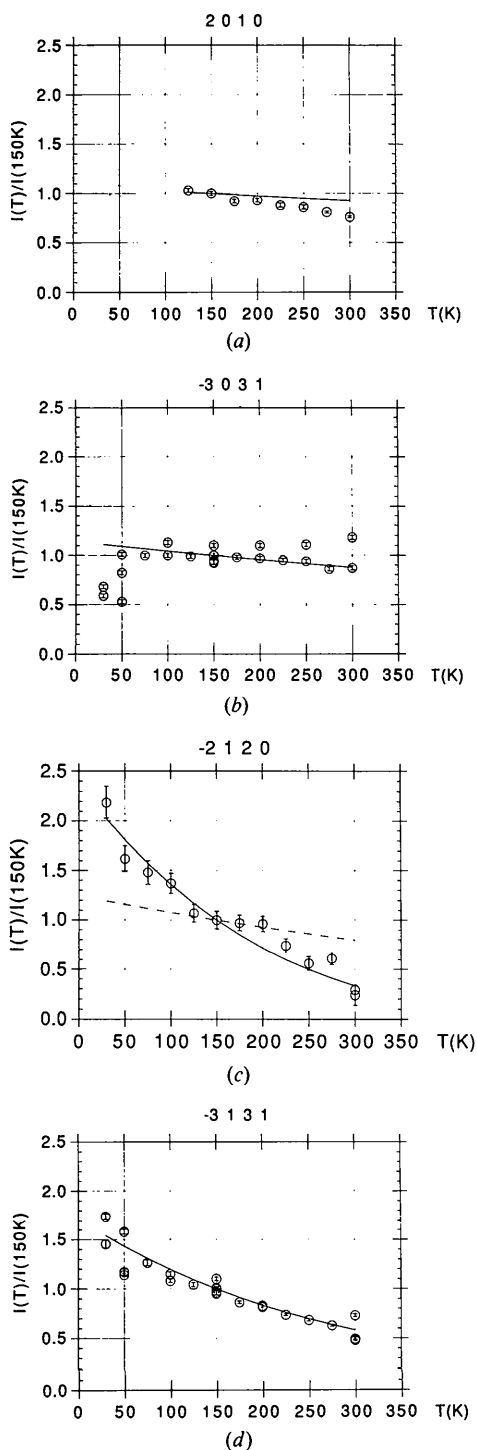
Fig. 4. Temperature dependence of the intensities of four reflections and the least-squares fit to the model including phason temperature factors. (a) 2010. (b) $\bar{3}031$. (c) $\bar{2}120$. (d) $\bar{3}131$. The last of these is a pure satellite reflection, the first a pure main reflection; the other two are mixed main–satellite reflections. Note that the indicated fit is based on a global four-parameter model and does not represent a fit to the individual reflection data points. The broken line in Fig. 4(c) is the fit obtained with a two-parameter Debye–Waller-coefficient-only model.

The corresponding value from the structure determination is $B_{Hg} = 2.3$ (1) Å^2. Because of the single-atom nature of the mercury sublattice and the expected small zero-point motion of the mercury atoms [Θ_D(Hg metal) = 100 K] (Ashcroft & Mermin, 1976), the agreement with the room-temperature B_{Hg} value supports the validity of the constant static-amplitude approximation. A decrease in the static distortion with increasing temperature (*i.e.* expanding lattices) would increase the primary reflection intensities and consequently would result in artificially low B values.

The non-negligible value of c_{Hg}^P implies significant phason excitation of the mercury sublattice at room temperature. The value of $c_{Hg}^P = 0.0026$ (2) $\text{rad}^2\,\text{K}^{-1}$ corresponds to a room-temperature r.m.s. phason fluctuation of $\langle\delta\varphi^2\rangle_{Hg}^{1/2} = (c_{Hg}^P \times 300)^{1/2} = 50$ (2)°. No comparable values are available in the literature, but Axe (1980) lists a range of 'plausible values' of $\langle\delta\varphi^2\rangle^{1/2}$ of $4 < \langle\delta\varphi^2\rangle^{1/2} < 57°$ for materials not subject to normal→incommensurate phase transformations. We note that the approximation made in (7b) is justified by this value of the phase fluctuations.

The observed temperature dependence of the phason fluctuations implies that the *mean* amplitude of displacement of the mercury atoms, η_{Hg}, will increase with decreasing temperature. The derived r.m.s. mercury fluctuation of 50° gives $(\eta/A)_{Hg} \simeq 1 - (\langle\delta\varphi^2\rangle_{Hg}/2) \simeq 0.6$, *i.e.* the mean amplitude of displacement of the Hg atoms is predicted to increase by about 60% on lowering of the temperature to near 0 K.

We conclude that the current study of the temperature dependence of the reflection intensities supports the existence of phason excitations in the mercury sublattice of the composite crystal of $Hg_{0.776}$ (BEDT-TTF)SCN.

References

Ashcroft, N. W. & Mermin, N. D. (1976). *Solid State Physics*, Saunders College, Table 23.3, p. 461. Philadelphia, PA: Holt, Rinehart and Winston.

Axe, J. D. (1980). *Phys. Rev. B*, **21**, 4181–4190.

Coppens, P., Cisarova, I., Bu, X. & Sommer-Larsen, P. (1991). *J. Am. Chem. Soc.* **113**, 5087–5089.

Graafsma, H., Sagerman, G. & Coppens, P. (1991). *J. Appl. Cryst.* **24**, 961–962.

Henricksen, K., Larsen, F. K. & Rasmussen, S. E. (1986). *J. Appl. Cryst.* **19**, 390–394.

Janner, A. & Janssen, T. (1980). *Acta Cryst.* A36, 399–408, 408–415.

OVERHAUSER, A. W. (1971). *Phys. Rev. B*, **3**, 3173–3182.

PEREZ-MATO, J. M. & MADARIAGA, G. (1990). *Geometry and Thermodynamics*, edited by J.-C. TOLEDANO, pp. 405–415. New York: Plenum Press.

PETRICEK, V., MALY, K., COPPENS, P., BU, X., CISAROVA, I. & FROST-JENSEN, A. (1991). *Acta Cryst.* A**47**, 210–216.

WANG, H. H., BENO, M. A., CARLSON, K. D., THORUP, N., MURRAY, A., PORTER, L. C., WILLIAMS, J. M., MALY, K., BU, X., PETRICEK, V., CISAROVA, I., COPPENS, P., JUNG, D., WHANGBO, M.-H., SCHIRBER, J. E. & OVERMYER, D. L. (1991). *Chem. Mater.* **3**, 508–513.

YAMAMOTO, A. (1982). *Acta Cryst.* A**38**, 87–92.

Patterson-Oriented Automatic Structure Determination. Deconvolution Techniques in Space Group *P*1

BY F. PAVELČÍK

Department of Inorganic Chemistry, Faculty of Natural Sciences, Comenius University, 842 15 Bratislava, Slovakia

Abstract

Several methods for the automatic determination of heavy-atom structures have been developed and extensively tested. The methods are based on a combination of vector superposition in space group *P*1 with a symmetry minimum function. The peaks of the symmetry minimum function are used as trial origin shifts in the translational search for the cell origin. Three or two Patterson shift vectors, all belonging to a single image, can be obtained for vector superposition by a procedure called cross-vector superposition. The superposition map may be refined by an automatic Fourier recycling in space group *P*1 before the translational search is started.

Introduction

Ab initio Patterson deconvolution techniques can be divided into two main groups depending on the utilization of symmetry:

(i) The symmetry is used from the very beginning and some atomic positions are suggested from the analysis of Harker regions (Harker, 1936) or more automatically using the multiple implication function (Simpson, Dobrott & Lipscomb, 1965). For more sophisticated techniques also using symmetry-related cross vectors, see Borisov (1964), Kuz'min, Golovachev & Belov (1970), Luger & Fuchs (1986), Pavelčík (1988) and Pavelčík, Kuchta & Sivý (1992).

(ii) The Patterson function is deconvoluted by a (weighted) vector minimum superposition (Buerger, 1959; Jacobson & Guggenberger, 1966) in space group *P*1 based on a carefully selected single Patterson vector or on several vectors all belonging to the same image. The symmetry is introduced after the structure has essentially been solved. Automatic structure determination based on vector minimum superposition in space group *P*1 has been reviewed by Simonov (1982). The general approach consists of several steps:

(1) Calculation of a (sharpened) Patterson function.

(2) Search for an atomic fragment using Patterson peaks or selection of a suitable Patterson peak for the superposition.

(3) Minimum-vector superposition.

(4) Inverse Fourier transform of modified minimum superposition map.

(5) Fourier recycling in space group *P*1.

(6) Search for a standard cell origin consistent with the space-group symmetry by some sort of translation function.

(7) Shift of the origin and electron-density averaging based on the symmetry.

(8) Fourier recycling using only peaks of the asymmetric part of the unit cell.

Even simplified algorithms based only on steps (1), (3) and (6) and the single vector superposition proved to be very successful in solving heavy-atom structures because of more sophisticated translation searching for multiple images (Richardson & Jacobson, 1987) or because of combination with the cross-vector table (Sheldrick, 1991; Sheldrick, Dauter, Wilson, Hope & Sieker, 1993).

The major sources of difficulty in the Simonov scheme are steps (2) and (6). The problem of selection of Patterson peaks may be overcome by a special superposition suggested by Iljukhin, Kuz'min & Belov (1981), which is called cross-vector super-